Dynamics of a Falling Particle Zone

TERRY L. CLARK AND ROLAND LIST

Dept. of Physics, University of Toronto, Ontario, Canada

(Manuscript received 19 June 1970, in revised form 1 March 1971)

ABSTRACT

A numerical experiment on falling particles arranged in zones, with slab symmetry, constant air density, and initially still air is performed whereby single-sized particles are treated by a Lagrangian method and the air motion by an Eulerian method.

The results of this study of the zone's dynamics indicate that the zones fall considerably faster than their respective terminal velocity. This additional or convective velocity depends on loading and terminal speed. The spreading velocities, away from the axis of symmetry, appear to be dependent on terminal velocity such that a maximum occurs near the terminal velocity of 4 m sec^{-1}.

In all cases considered, the magnitude of the perturbation nonhydrostatic pressure gradient in the vertical is found to be an order of magnitude smaller than the perturbation hydrostatic pressure gradient.

1. Introduction

Some of the factors which can affect the distribution of precipitation-sized particles within a cloud are coalescence, breakup, sedimentation, and gravitational feedback effects. It is the two latter factors with which this paper will be concerned. As a first attempt, two-dimensional zones of single-sized particles falling in still air will be discussed using a numerical model. Coalescence and breakup will be ignored so that the fall pattern and the flow created by the falling particles can be isolated, which makes the study less complicated and its conclusions easier to understand.

Previous work in this area restricted to one-dimensional models includes that of Das (1964), where the formation of a downdraft caused by liquid water loading was investigated. Takeda (1966) studied the formation of a downdraft in which the drag and evaporation of raindrops were taken into account. Srivastava (1967) employed some suggestions by Kessler (1963) of a simple way of treating precipitation. In all these models, the drag of the liquid water was included in the vertical equation of motion, with horizontal pressure surfaces assumed. Lozowski and List (1969) found, through two-dimensional numerical experiments, that the magnitude of the pressure gradient in the vertical (they exclude the hydrostatic pressure gradient caused by the air at infinity) is of the same order of magnitude as the drag effects, when considering a steady state of a large particle zone. Their results suggest that the assumption of horizontal pressure surfaces, which are inherent in one-dimensional cloud models, is not adequate.

Two-dimensional cloud models such as employed by Árnason *et al.* (1968), Liu and Orville (1968) and Takeda (1965) include the nonhydrostatic pressure gradients when modelling the drag effects of liquid water. Árnason *et al.* and Liu and Orville were concerned with cumulus-scale convection and Takeda with wind-shear effects on cumulonimbus clouds. However, the present authors feel that the existing two-dimensional cloud models, in an attempt at realism, have become too complicated and include too many different aspects to learn much about any single effect. For this reason, a rather primitive example of a falling particle zone is presented in order to learn how the precipitation particles affect the air's motion and their own relative motion. Attention will be paid to the numerical method in order to suppress as many undesirable non-physical effects of the mathematics as possible, such as numerical damping caused by the finite-difference scheme for the advection of precipitation particles.

2. Governing equations and boundary conditions

A two-dimensional atmosphere with slab symmetry and constant air density is assumed. The depth of the atmosphere will be taken as 10 km with an effect similar to that produced by the ground and tropopause simulated through the lower and upper vertical velocity boundary conditions, i.e., the vertical velocity will be made to vanish at heights of 0 and 10 km. Precipitation particles and dry air will be the only substances considered, and all particles will be of the same size and terminal velocity for any particular example.

The precipitation particles are assumed to move with the air in the horizontal and fall at terminal velocity relative to the air in the vertical. If an analysis similar to Kessler's (1967) is carried out for large particles (such as hailstones) with terminal velocities of the order of 16 m sec^{-1}, one finds the following: 1) the particles originally at rest attain 99% of their terminal

velocity after approximately 4 sec, and 2) they have 99% of the horizontal wind velocity after approximately 8 sec. These times are two orders of magnitude smaller than the time constant for the air's motion.[1] This assumption is even better justified for smaller particles. Thus, one is justified in using the steady-state conditions for relative motion of the particles with respect to the air. (Slip velocities will also be neglected.) It will be *assumed* then, that the *particles exert their weight on the air in the vertical and exert no force on the air in the horizontal.*

An eddy viscosity is assumed for the equations of air motion but not for the relation governing the advection of precipitation particles.

The present purpose in using an eddy viscosity for the equations of air motion is mainly for computational reasons. A constant eddy viscosity of 1000 m^2 sec^{-1}, it is felt, will damp large amounts of wind shear which would lead to unreasonably large truncation errors for a numerical grid size of 500 m square. Mixing of the precipitation particles is not modelled because of the desire to determine the flow characteristics of a falling zone without modelled turbulence. Future work, with turbulence modelled for the particles, will be easier to analyze by comparison of results. An attempt will be made to estimate the effect of the eddy viscosity on the motion of the particles.

The governing equations to be used are

$$\frac{\partial w}{\partial t}+\frac{\partial (uw)}{\partial x}+\frac{\partial (ww)}{\partial z}=-\frac{\partial \phi}{\partial z}-gr+\nu_e\nabla^2 w, \quad (1)$$

$$\frac{\partial u}{\partial t}+\frac{\partial (uu)}{\partial x}+\frac{\partial (uw)}{\partial z}=-\frac{\partial \phi}{\partial x}+\nu_e\nabla^2 u, \quad (2)$$

$$\frac{\partial u}{\partial x}+\frac{\partial w}{\partial z}=0, \quad (3)$$

$$\frac{\partial r}{\partial t}+\frac{\partial (ru)}{\partial x}+\frac{\partial}{\partial z}[r(w-V_T)]=0, \quad (4)$$

where (1) and (2) describe the vertical and horizontal air motion, (3) the mass continuity, and (4) the conservation of liquid water; and where w and u are the vertical and horizontal wind speeds, r the water substance mixing ratio, V_T the terminal velocity (assumed constant), ν_e the eddy viscosity (assumed constant), g the acccleration due to gravity, x, z and t the horizontal and vertical distances and time, and ϕ the pressure over density ratio plus gz.

Other terms which will be used when referring to (1) and (2) are the perturbation hydrostatic pressure and the perturbation nonhydrostatic pressure. The perturbation hydrostatic pressure at a point will be taken to mean the total weight of water substance above that point per unit area. The perturbation nonhydrostatic pressure will then be used to mean the total pressure minus the perturbation hydrostatic pressure. Since the fluid considered is incompressible, it is convenient to link the definition of the perturbation nonhydrostatic pressure directly with the hydrometeor drag [List and Lozowski (1970) related it to air density perturbation and did not convert hydrometeor drag into a pressure gradient].

The boundary conditions which will be used are

$$\frac{\partial w}{\partial x}=u=\frac{\partial \phi}{\partial x}=0 \quad \text{at } x=0 \text{ and } 10 \text{ km}, \quad (5)$$

$$\frac{\partial u}{\partial z}=w=\frac{\partial \phi}{\partial z}=0 \quad \text{at } z=0 \text{ and } 10 \text{ km}. \quad (6)$$

Eq. (5) implies an axis of symmetry at $x=0$ and a frictionless "wall" at $x=10$ km. Eq. (6) implies frictionless walls at $z=0$ and $z=10$ km. Welch *et al.* (1966) suggest that frictionless boundary conditions are justified as long as the surface boundary layer is very much smaller than the grid size. Since the vertical grid size is 500 m it seems justifiable to treat the ground as a frictionless surface.

A particle zone 4 km wide by 2 km deep, with an initially uniform mixing ratio ranging from 0.008–0.010, will be centered about the $z=8$ km and $x=0$ km position. The air is initially still and the zone of particles is allowed to fall freely at terminal velocity with respect to the air after the time of release.

3. Convective velocity of the particle zone

The equation for the conservation of energy which corresponds to (1)–(6) is

$$\frac{\partial}{\partial t}\int\int[\tfrac{1}{2}(u^2+w^2)+grz]dxdz=-\int\int grV_T dxdz$$

$$-\nu_e\int\int\left[\left(\frac{\partial u}{\partial x}\right)^2+\left(\frac{\partial u}{\partial z}\right)^2+\left(\frac{\partial w}{\partial x}\right)^2+\left(\frac{\partial w}{\partial z}\right)^2\right]dxdz, \quad (7)$$

which we rewrite as

$$\frac{\partial K}{\partial t}+g\frac{\partial (QZ)}{\partial t}=-gV_TQ-D, \quad (8)$$

where

$$\left.\begin{aligned} K&=\int\int\tfrac{1}{2}(u^2+w^2)dxdz \\ Q&=\int\int rdxdz, \quad QZ=\int\int rzdxdz \\ D&=\nu_e\int\int\left[\left(\frac{\partial u}{\partial x}\right)^2+\left(\frac{\partial u}{\partial z}\right)^2+\left(\frac{\partial w}{\partial x}\right)^2+\left(\frac{\partial w}{\partial z}\right)^2\right]dxdz \end{aligned}\right\}.$$

[1] Height$\times$(terminal velocity)$^{-1}$=(10 km$\times$16 m sec^{-1})$^{-1}\approx$600 sec.

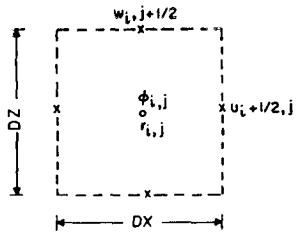

FIG. 1. Placement of variables on the Eulerian grids.

If Q is assumed constant, which is the case when no precipitation has reached the ground, then (8) can be rewritten as

$$V_c=\left(\frac{\partial Z}{\partial t}+V_T\right)=-\frac{1}{gQ}\left(\frac{\partial K}{\partial t}+D\right), \tag{9}$$

where V_c is the convective velocity of the center of mass of the particle zone, Z the vertical position of the zone's center of mass, $\partial K/\partial t$ the rate of increase of the air's energy over density, D the energy dissipation term, and Q the total amount of particles.

Eq. (9) allows a crude test of the importance of the eddy viscosity in moving the precipitation particles. The ratio of the area of the zone to the area of the zone plus its "wake" (approximately equal to fall height times zone diameter) will be used to estimate the proportion of the total dissipation which occurs in the zone region. It will be assumed that the above-mentioned ratio times D gives us the proportion of dissipation, d, which is contributing to slowing down the zone, i.e.,

$$d=\left[\frac{h}{h+(|V_c|+V_T)t}\right]D, \tag{10}$$

where h is the characteristic height of the particle zone. The above argument essentially assumes that the smaller scales of motion in the wake, where dissipation is significant, are approximately unaffected by the zone below. Dissipation in the small scales is assumed uniform in space. If $|d/(gQV_c)|\ll 1$, then V_c depends on the inertial terms of the equations and it is assumed that the eddy viscosity is not playing a major role in moving the particle zone. The above test will only be considered while the zone is well above the ground. Once the particle zone approaches the ground, the boundary conditions will dominate the motion and V_c will approach zero.

Eq. (9) implies that the kinetic energy changes of the particles of the particle zone are neglected. The sum of the kinetic energy of the air, K, and the potential energy of the zone, $gQ(Z+V_Tt)$, could be looked upon as the mechanical energy of the system. This energy will be changed only by dissipation due to the eddy viscosity. If the zone would fall at the terminal velocity of the particles, there would be no production of kinetic energy of the air and no particle zone acceleration since the particle weight would be compensated by the vertical pressure gradient. An example would be an infinite homogeneous layer in the horizontal.

4. Numerical method

Eqs. (1)–(6) are solved using a mixed Eulerian-Lagrangian method. The Eulerian grid consists of 22 by 22 grids, each grid 500 m square. The positioning of the variables is shown in Fig. 1. The vertical boundaries will correspond to w positions and the horizontal boundaries to u positions. This makes it a simple matter to put the normal velocities to zero at the boundaries. If i and j designate the horizontal and vertical positions, respectively, of the (i, j) grid, we have

$$\left.\begin{aligned} x&=(Dx/2)+(i-2)Dx\\ z&=(Dz/2)+(j-2)Dz \end{aligned}\right\} \tag{11}$$

at the grid center, where Dx and Dz are the horizontal and vertical grid lengths.

The particle mixing ratio will be initially represented by 25 tracer particles in each cell which contains precipitation particles. Each tracer will then represent a mixing ratio of $r_0/25$, where r_0 is the initial mixing ratio.

The numerical procedure is summarized as follows:

1) Set up initial fields.
2) Move all tracer particles a distance given by

$$\Delta z_k=(w_k-V_T)DT,$$

$$\Delta x_k=u_kDT,$$

where k refers to the kth tracer particle, w_k and u_k are determined by a linear average of the four nearest w and u values, and DT is the time increment (usually 12.5 sec).

3) Sum the number of tracer particles in each grid to determine the new mixing ratio r.

4) Using all the present Eulerian fields for u, w, r and ϕ, solve for the new ϕ values.

5) Using Eqs. (1) and (2) in numerical form, find the new values for u and w.

6) Go back to step 2) and repeat the cycle.

The method used to solve for u, w and ϕ is that described by Harlow and Welch (1965). Initial "random" positioning of the tracer particles was not used because there were enough tracer particles involved so that the problem of "surges," caused by a row of particles all passing a grid boundary together, did not warrant attention. Also, the method used to assign velocities to the particles would, to a large extent, stop any large surges, i.e., the velocity field is treated as continuous as far as the tracer particles are concerned. A test run with the tracer particles initially staggered showed no significant change in the solution from that obtained

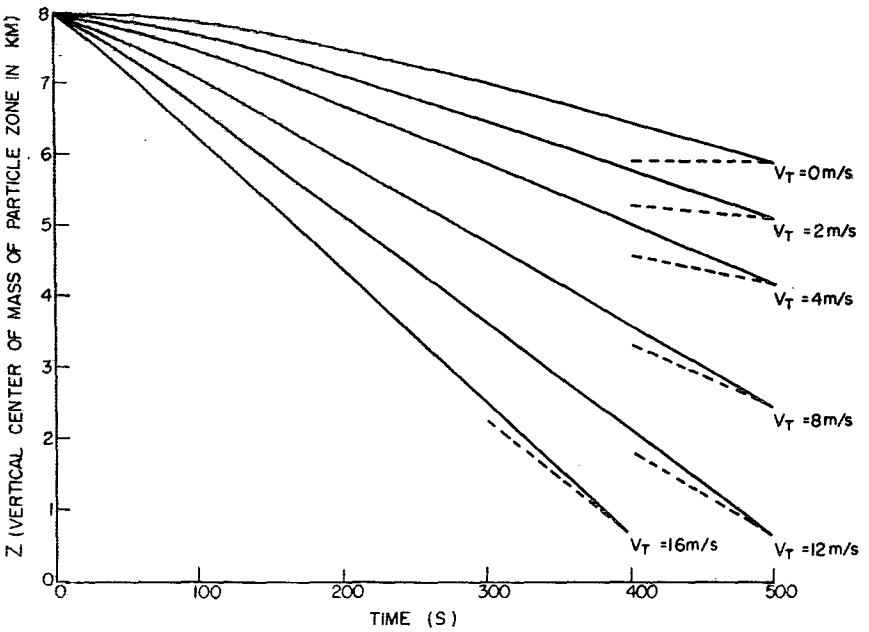

FIG. 2. Vertical position of the center of mass of zones as a function of time for various terminal velocities V_T. Dashed lines represent slopes which correspond to the respective terminal velocities. The initial mixing ratio was 10 gm kg^{-1}.

by having the tracer particles initially in rows and columns.

The Lagrangian technique for moving the precipitation particles was used instead of an Eulerian method, such as an upstream differencing method, for two reasons: first, the Lagrangian method is easily adapted to zones of different sized particles without having to assume an averaged terminal velocity field; and, second, an Eulerian technique would treat motion near the particle zone boundaries rather badly. It is at these boundaries where the major portion of vorticity is produced which redistributes the falling particles relative to one another. Thus, one would be rather hesitant in attributing observed flow characteristics to the physics instead of the mathematics if an Eulerian advection method were used.

A comparison of results for a falling zone was made using first an upstream differencing technique and then the above-mentioned Lagrangian method. The comparison indicated that the upstream differencing method not only treated advection at the particle zone boundaries differently but also produced much weaker gradients of precipitation particle mixing ratio. Another major difference was the early loss of water from the Eulerian system through precipitation.

5. Results

Fig. 2 is a plot of the vertical distance to the center of mass of the entire particle zone as a function of time. The six cases considered are for terminal velocities of 0, 2, 4, 8, 12 and 16 m sec^{-1}. In all cases the particle zone was stationary at time zero and the initial aspect ratio of the zone was 2, where the aspect ratio is defined as the horizontal length over the vertical depth. The initial mixing ratio was 0.01 throughout the zone. After a constant velocity has been reached it is observed that the magnitudes of the velocities are considerably in excess of the respective terminal velocities. This excess of fall velocity is called the convective velocity of the particle zone. Fig. 3 shows that the convective velocity depends not only on loading but also on terminal velocity. The two curves indicate that the importance of loading decreases with increasing terminal velocity, since at $V_T = 12$ m sec^{-1} there is a difference of only 0.2 m sec^{-1}

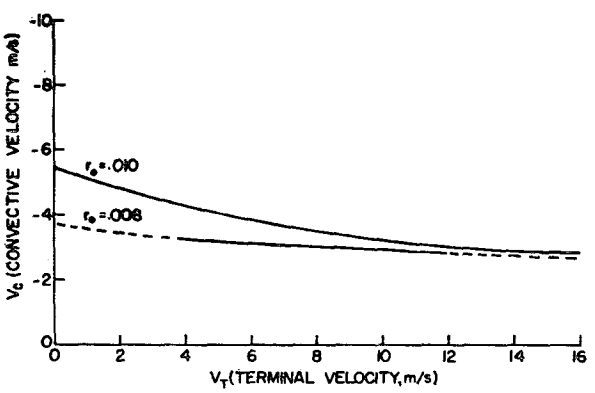

FIG. 3. Convective velocity V_c vs terminal velocity V_T for two initial mixing ratios (gm gm^{-1}). Values of V_c were determined from the slope of curves such as those in Fig. 2. The initial position and dimensions of all zones were equal.

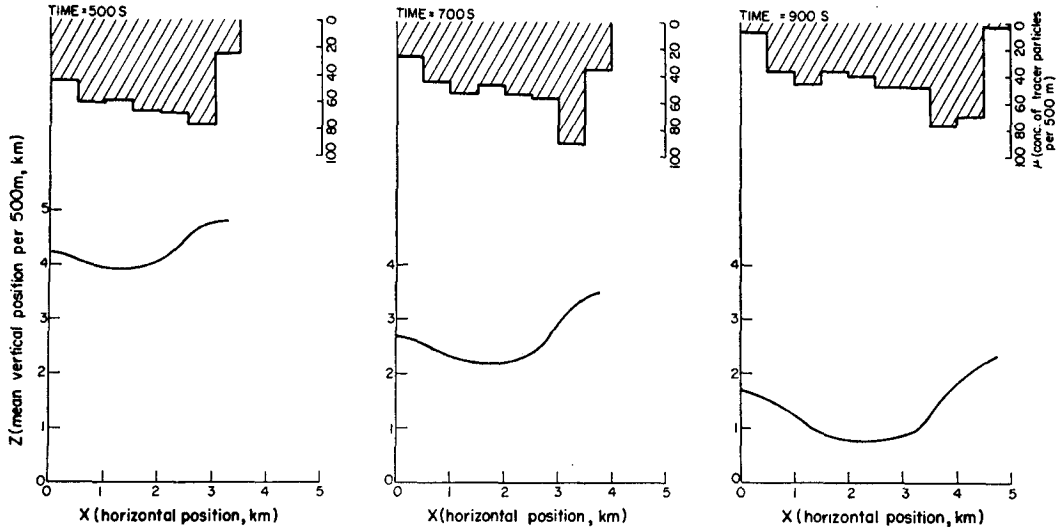

FIG. 4. Mean vertical position of the zone as a function of the horizontal displacement from axis of symmetry at various times. The hatched section shows the concentration of tracer particles per 500 m width; $V_T=4$ m sec^{-1}.

in V_c between $r_0=0.01$ and 0.008, compared with a difference of 1 m sec^{-1} at $V_T=4$ m sec^{-1}. The curves do not extend to values of terminal velocity >16 m sec^{-1} because of the large amount of computation required due to an increasingly smaller time step.

The circulation that is produced in the air by the falling zone gives the zone its convective velocity. This air motion redistributes the falling particles relative to one another. As the particles fall a double minimum in the horizontal profile of the air's vertical velocity forms. This profile causes the particle zone to fall faster approximately midway between the axis of symmetry and the zone's outer boundary. Fig. 4 is a plot of the zone's average vertical position as a function of time and horizontal distance. The initial mixing ratio is 0.01 and the terminal velocity 4 m sec^{-1}. As the zone approaches the ground a considerable horizontal variation has developed in the vertical position of the zone. Also apparent from Fig. 4 is the large amount of horizontal advection of the falling particles. At 900 sec the region near the axis of symmetry has been almost completely depleted of falling particles.

Fig. 5 consists of two-dimensional plots of the w, u, and ϕ fields at 125-sec intervals. At 250 sec the double minimum horizontal profile of the w field, within the particle zone, becomes apparent. This profile of w persists until the zone reaches the ground. At 750 sec no particles have reached the ground but precipitation starts in $\sim$50 sec.

The zone falls in such a way that initially there is positive u in the lower regions of the zone and negative u in the upper regions. After 250 sec there are only positive u values within the zone. This causes considerable horizontal advection of the particles. The horizontal boundary of the zone has gone from its initial value of 2 km to almost 5 km at 750 sec.

The mean horizontal positions of the particle zones were calculated every 12.5 sec up to and including 400 sec. A relatively constant horizontal velocity occurred for the mean horizontal position of the zone after sufficient time integration. This horizontal velocity is called the mean spreading velocity and was calculated for initial mixing ratios of 0.01 and terminal velocities of 0, 4, 8, 12, 16 and 20 m sec^{-1}. The respective spreading velocities were 1.6, 2.18, 1.85, 1.65, 1.45 and 1.2 m sec^{-1}. The spreading velocity has a rather interesting maximum in the region of 4 m sec^{-1} terminal velocity. It is suggested that the decrease in the spreading velocity with decreasing V_T ($\lesssim 4$ m sec^{-1}) is caused by the zone's decreasing ability to fall out of the region of negative horizontal air velocities.

An analysis of the ϕ field suggests that $\partial\phi/\partial z \approx -gr$ within the particle zone. This implies that the resulting vertical force on the air in the region of the particle zone is considerably smaller than the particle weight. Thus, the vertical accelerations of the air in the zone region are considerably smaller than one might expect from a simple dimensional argument where horizontal pressure surfaces were assumed. The terms containing the pressure gradient term and particle weight in the vertical equation of motion were both horizontally integrated from the axis of symmetry to the outermost boundary position of the particle zone. This was done at each z level and at three different times. Fig. 6 is a plot of the various resulting terms. The solid line is the integral of gr and the heavy dashed line the integral of $\partial\phi/\partial z$. The light dashed line is the sum of the previous two integrals and thus represents the perturbation nonhydrostatic pressure term. The perturbation hydro-

static pressure gradient, which is the negative of the particle weight term, is over ten times larger than the perturbation nonhydrostatic pressure term in the regions of heavy particle concentration. The sum of the first two terms on the right-hand side of (1), in the region of heaviest particle concentration, is a magnitude smaller than the magnitude of either of the terms for all cases treated to date, i.e.,

$$\left|\int_0^{x_1}\left(\frac{\partial\phi}{\partial z}+gr\right)dx\right|\leqslant\frac{1}{10}\int_0^{x_1}grdx, \qquad (12)$$

where x_1 represents the outermost boundary of the particle zone.

Time integration of the equations was continued until all the particles had reached the ground. Fig. 7 shows the distribution of particles on the ground after 100% precipitation. Also displayed is the initial distribution of vertically integrated tracer particles. Again the terminal velocity is 4 m sec^{-1} and the initial mixing ratio 0.01. The density of tracer particles on the ground ranges from 38–28 (500 m)$^{-1}$ in the region of significant precipitation. Sharp cutoffs in tracer par-

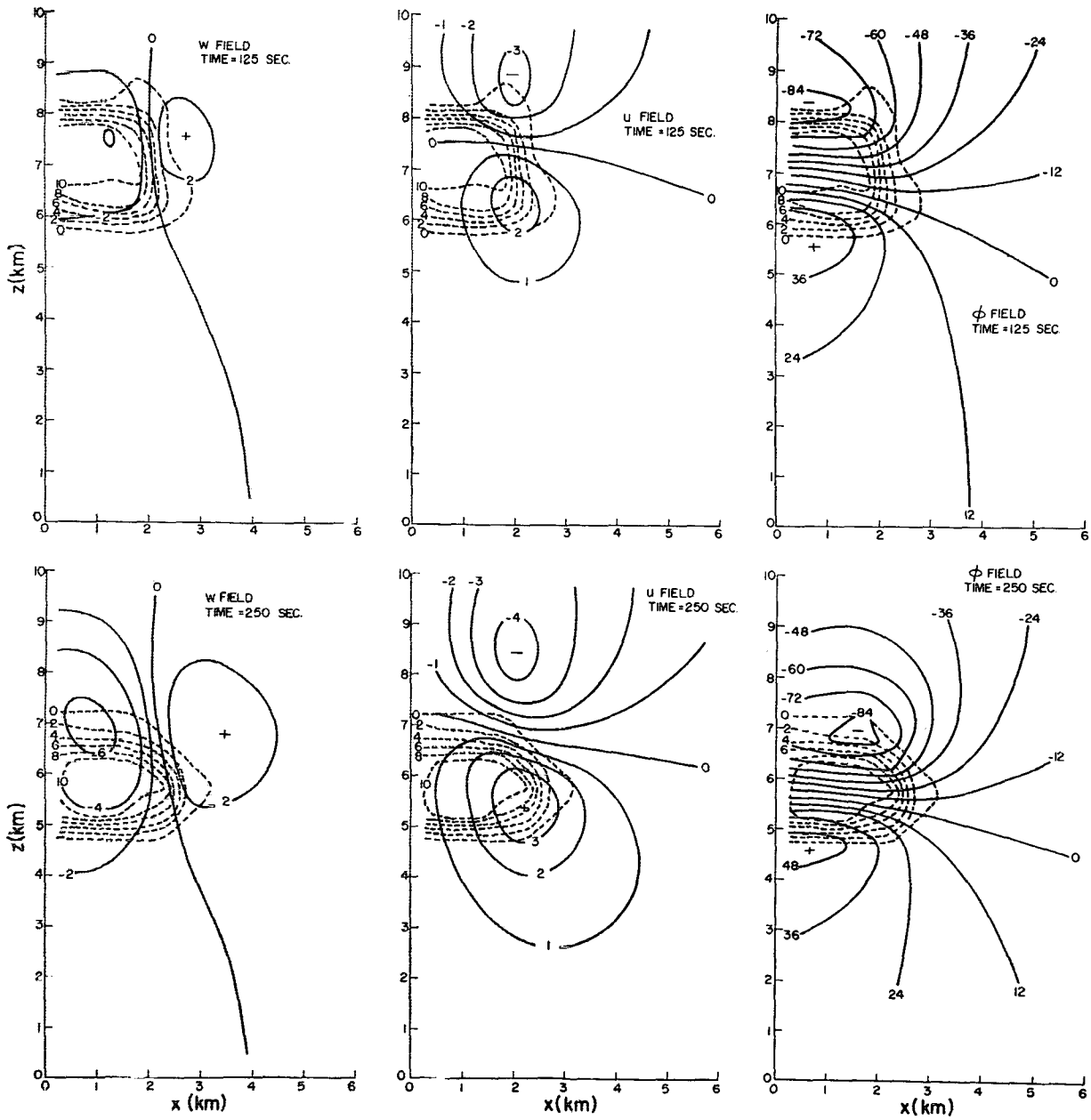

FIG. 5. Two dimensional plots of u and w (m sec^{-1}), ϕ (m^2 sec^{-2}) [all solid lines] and r (gm kg^{-1}) [dashed lines] at various times. The contour interval for ϕ corresponds to 0.12 mb if the air density is taken as 1 kg m^{-3}; V_T=6 m sec^{-1}.

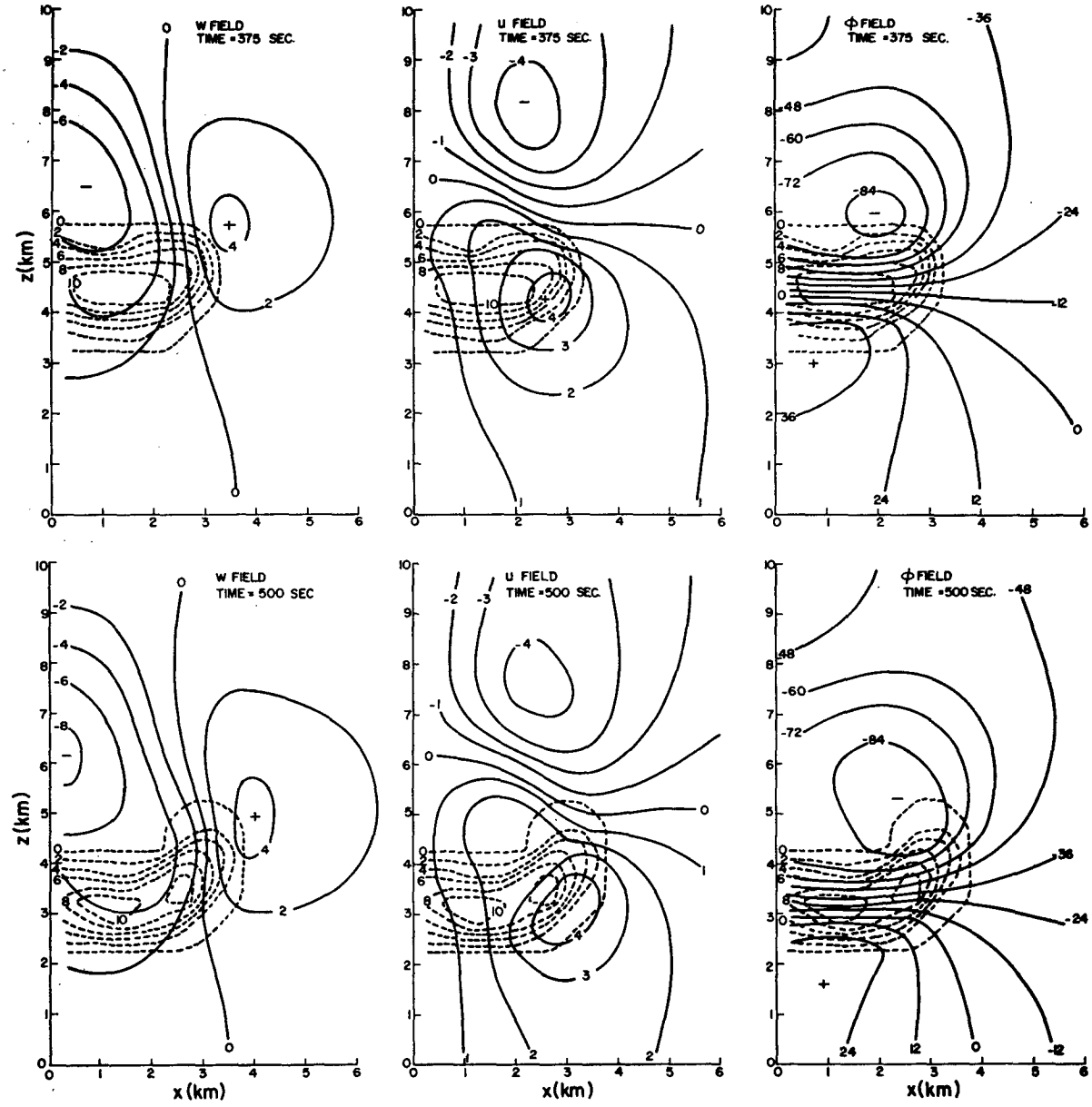

FIG. 5. (*continued*)

ticle density appear at the outer region and also near the axis of symmetry. The "hole" which is produced at the axis of symmetry implies that the tracer particles nearest the axis have been advected from their initial position of 83 m to over 500 m. The use of more tracer particles would result in the filling of this hole but the relative density would still be very low.

To ensure that the $x=10$ km was not affecting the results to an appreciable extent the boundary was extended to 20 km for one run. A comparison of the results showed no significant changes.

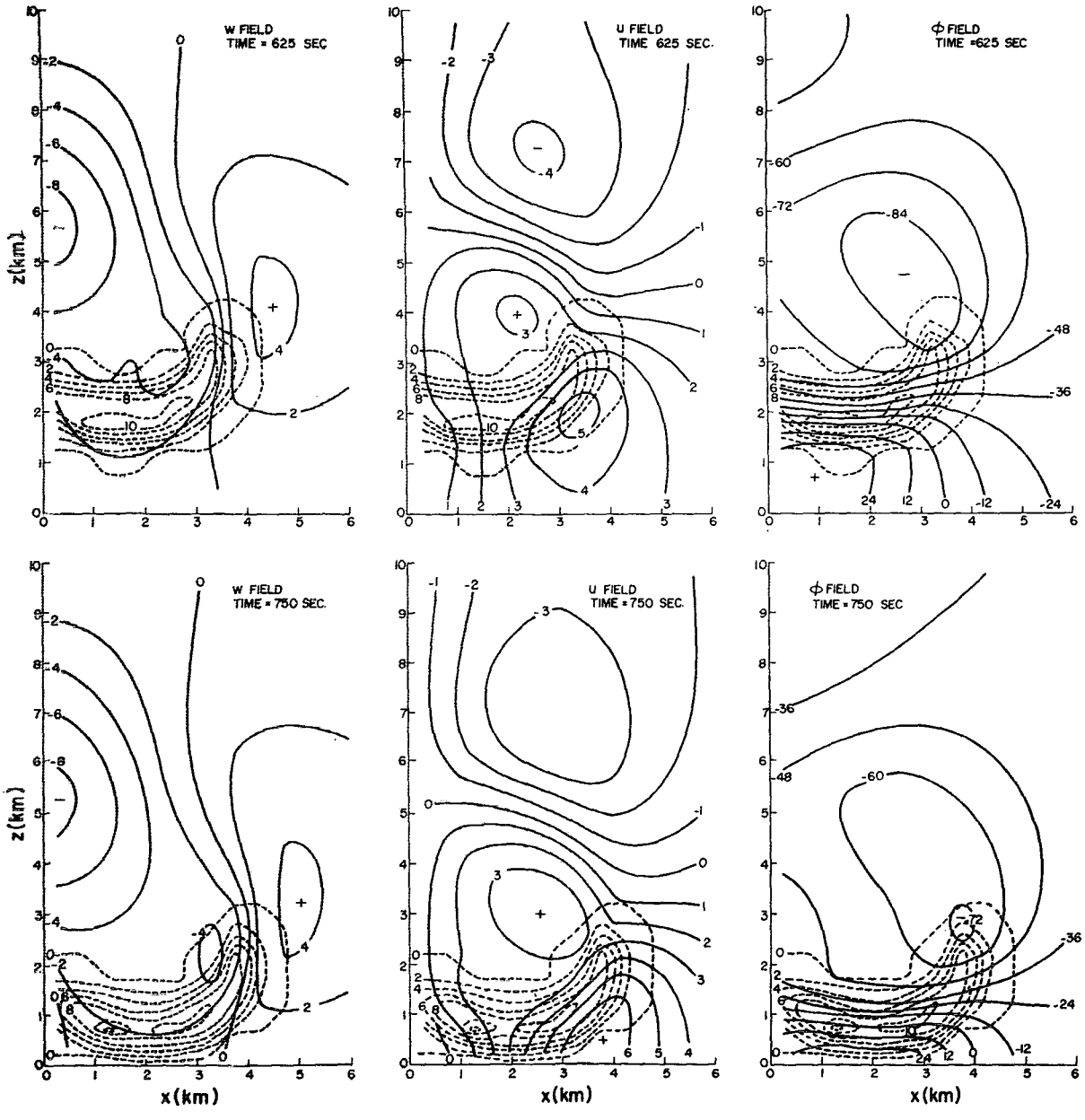

FIG. 5. *(continued)*

6. Effect of eddy viscosity

A plot of $|d/(gQV_c)|$ for terminal velocities of 0, 2, 4 and 16 m scc^{-1} with $r_0=0.01$ in Fig. 8 shows that the eddy viscosity has contributed less than 11% to the convective velocity of the falling zone for terminal velocities $\gtrsim 4$ m sec^{-1}. Below 4 m sec^{-1} the importance of the eddy viscosity becomes only slightly larger. It should be remembered that these curves are based on a very simple theory and are meant only to give a very rough idea of the importance of the eddy viscosity. If the effect is low this means one has effectively looked

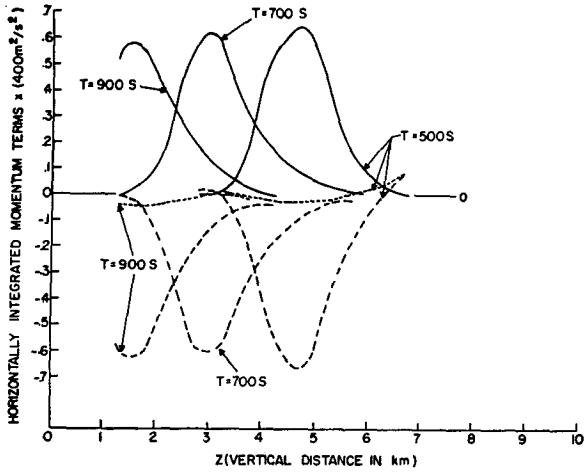

FIG. 6. Height variation of the horizontally integrated values of gr for different times (solid lines). Heavy dashed lines represent $\int(\partial\phi/\partial z)dz$, taken between $0\leqslant x\leqslant x_1$, as a function of z, and light dashed lines the difference between the two terms, i.e., the integral of the perturbation nonhydrostatic pressure. The initial zone size is as in Fig. 5; $V_T=4$ m sec^{-1}; $r_0=0.01$ gm gm^{-1}.

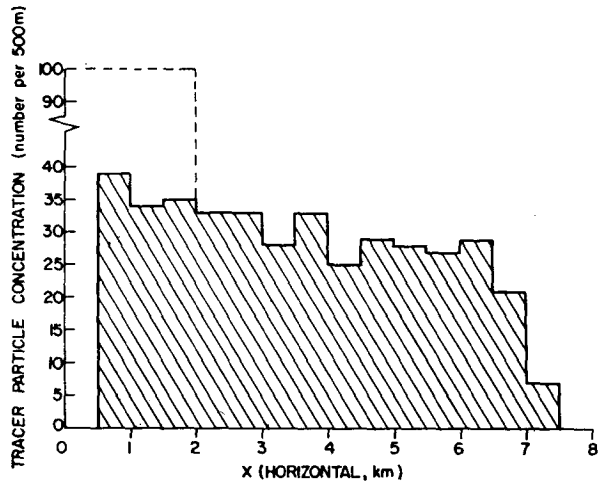

FIG. 7. Distribution of tracer particles on ground after 100% precipitation, for $V_T=4$ m sec^{-1} and initial mixing ratio $r_0=0.010$ gm gm^{-1}. The dashed line represents the initial distribution.

at the nonturbulent characteristics of a falling particle zone, which seems to be the case.

The eddy viscosity was increased from 1000 to 2000 m^2 sec^{-1} for a falling zone of terminal velocity 4 m sec^{-1} and initial mixing ratio of 0.01. There was no detectable change in the mean vertical motion. Both runs had identical convective velocities. This indicates that the curves in Fig. 8 are an overestimate of the effect of the eddy viscosity on the mean vertical motion of the zone. One noticeable effect which did occur by doubling the eddy viscosity was that the double minimum, in the horizontal, of the vertical position of the zone (as in Fig. 4) was less prominent, i.e., the relative motion of the particles was slightly affected by increasing the eddy viscosity.

7. Energy balance

Each computer run was checked for conservation of mass, momentum and energy. The energy balance was checked through Eq. (9). At each time step, values were determined for K, V_c and D. After 40 time steps the final K was determined by the integration of (9) using the collected values of V_c and D. It was found that the calculated values of K and actual K differed by less than 1.5%. The discrepancy increased proportionately for longer periods of time (750 sec in Fig. 5 corresponds to 60 time steps).

8. Conclusions

The results indicate that the rather unorthodox use of an eddy viscosity in the momentum equations and not in the advection equation for the particle zone did not affect the calculations appreciably. Thus, the results presented can be assumed to visualize the nonturbulent case of a falling particle zone. While incorporation of a mixing process for the particles into the system would put the eddy viscosity in the momentum equations on firmer physical grounds, the physical nature of the mixing process for precipitation particles

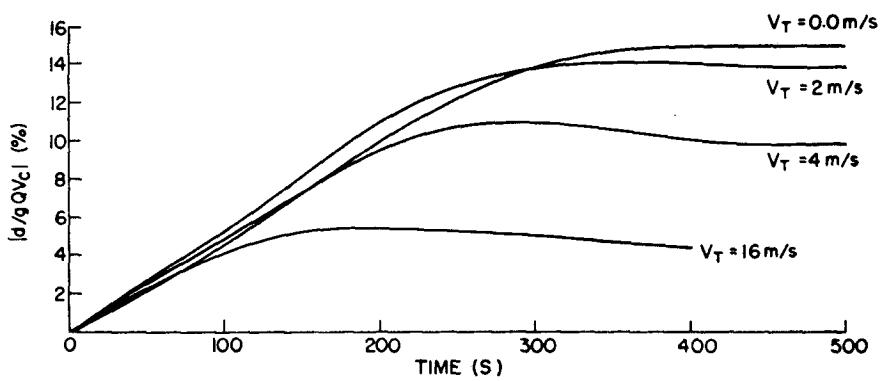

FIG. 8. Estimated effect of the eddy viscosity on the convective velocity of the falling zones as a function of time for various terminal velocities V_T; $r_0=0.01$ gm gm^{-1}.

is at present unknown to the authors. Results with mixing could then be compared to those without, to get a reasonable evaluation of its effect.

It was found that the *mean vertical motion of the particle zone depends on both total water substance weight and the zone's terminal velocity.* The magnitude of the convective velocity was approximately equal to that of the terminal velocity for 4 m sec^{-1} particles. For smaller particles, $|V_c| > V_T$, and for larger particles, $|V_c| < V_T$. The critical value for the velocity may be different for $r_0 \neq 0.01$.

A significant double minimum, in the horizontal, of the vertical position of the zone was observed to occur for all values of terminal velocity and loading considered. Introduction of a mixing process for the particles would likely either diminish this effect or completely alter it.

An important observation, in all cases considered, was that *the vertical pressure gradient was within 10% of the perturbation hydrostatic pressure gradient caused by precipitation particle weight.* This indicated that the falling zone does not affect the vertical momentum of the air to the extent to which one might expect from a simple dimensional argument where horizontal pressure surfaces are assumed.

The production of horizontal momentum within all regions of the particle zone caused considerable advection of particles away from the axis of symmetry. Introduction of a particle mixing process may fill the hole to some extent but is unlikely to reduce the amount of mass advected away from the axis of symmetry. An interesting aspect of the *spreading velocity*, for the zones treated, is the *maximum* which occurs for $r_0 = 0.010$ in the region of 4 m sec^{-1} terminal velocity. This maximum, it is felt, is caused by the zone's decreasing ability to fall out of the region of negative horizontal air velocities with V_T decreasing below 4 m sec^{-1}.

The authors realize that many of the assumptions made should be relaxed before the present results can be considered conclusive. This paper was intended as a first attempt in the understanding of falling particle zones. It is felt (personal communication by H. K. Weickmann) that the results may have applications to mammatus.

Acknowledgments. This work was carried out within a research program sponsored by the Meteorological Service of Canada and by the Environmental Science Services Administration of the U. S. Department of Commerce, through the National Severe Storms Laboratory, Norman, Okla. One of the authors (T. L. C.) is indebted to the Blyth Foundation for a scholarship received through the University of Toronto.

REFERENCES

Árnason, G., R. S. Greenfield and E. A. Newburg, 1968: A numerical experiment in dry and moist convection including the rain stage. *J. Atmos. Sci.*, **25**, 404–415.

Das, P., 1964: Role of condensed water in the life cycle of a convective cloud. *J. Atmos. Sci.*, **21**, 404–418.

Harlow, F. H., and J. E. Welch, 1965: Numerical calculation of time-dependent viscous incompressible flow of fluid with free surface. *Phys. Fluids*, **8**, 2182–2189.

Kessler, E., 1963: Elementary theory of associations between atmospheric motions and distributions of water content. *Mon. Wea. Rev.*, **91**, 13–27.

---, 1967: On the continuity of water substance. Institutes for Environmental Research, Tech. Memo. IERTM-NSSL 33.

List, R., and E. P. Lozowski, 1970: Pressure perturbations and buoyancy in convective clouds. *J. Atmos. Sci.*, **27**, 168–170.

Liu, J. Y., and H. D. Orville, 1968: Numerical modelling of precipitation effects on a cumulus cloud. Inst. Atmos. Sci., Rept. 68–9, South Dakota School of Mines and Technology.

Lozowski, E. P., and R. List, 1969: Updraft divergence associated with hydrometeor drag: A numerical computation. *Preprints of Papers, Sixth Conf. Severe Local Storms*, Chicago, Amer. Meteor. Soc., 55–58.

Srivastava, R. C., 1967: A study of the effect of precipitation on cumulus dynamics. *J. Atmos. Sci.*, **24**, 36–45.

Takeda, T., 1965: The downdraft in convective shower-cloud under the vertical wind shear and its significance for the maintenance of convective system. *J. Meteor. Soc. Japan*, **43**, 302–309.

——, 1966: The downdraft in the convective cloud and raindrops: A numerical calculation. *J. Meteor. Soc. of Japan*, **44**, 1–11.

Welch, J. E., F. H. Harlow, J. P. Shannon and B. J. Daly, 1966: The MAC method. Rept. LA-3425, Los Alamos Scientific Laboratory.